## Reconciling solar and terrestrial neutrino oscillation evidences with minimum sacrifice

G. L. Fogli, E. Lisi, D. Montanino, and G. Scioscia Dipartimento di Fisica and Sezione INFN di Bari, Via Amendola 173, I-70126 Bari, Italy

### Abstract

The present possible evidences in favor of neutrino masses and mixings from solar, atmospheric, and accelerator experiments cannot be all reconciled in a three-family framework, unless some data are excluded. We grade all possible three-family scenarios according to their compatibility with the available data. A recently proposed scenario appears to emerge naturally as the most likely solution to all oscillation evidences, with the only exception of the angular dependence of multi-GeV atmospheric data in the Kamiokande experiment. We describe in detail the status and the phenomenological implications of this "minimum sacrifice" solution.

PACS number(s): 14.60.Pq, 26.65.+t, 95.85.Ry, 13.15.+g

#### I. INTRODUCTION

At present, there are three possible evidences for neutrino masses and mixings: the solar neutrino problem [1], the atmospheric neutrino anomaly [2], and the event excess in the Liquid Scintillator Neutrino Detector (LSND) experiment [3]. These evidences are individually best-fitted by three largely different mass gaps in the neutrino spectrum, and thus cannot be all reconciled in a three-flavor  $(3\nu)$  oscillation framework, unless some data are excluded (see, e.g., [4]).

In this work we grade all possible three-flavor scenarios according to their compatibility with the world neutrino data. The specific data conflicting with the various scenarios are systematically identified. We treat in increasing detail those  $3\nu$  frameworks that require a decreasing "sacrifice" of data in order to achieve a good global fit. The scheme recently proposed by Cardall and Fuller [5] will emerge as the "minimum sacrifice" scenario, and its implications for current and future experiments will be investigated in detail. In developing our analysis, we also comment on other three-flavor analyses recently appeared in the literature [6–9]. This work builds upon our previous studies of solar [10,11], atmospheric [12,13], and laboratory (accelerator and reactor) [14,15] neutrino oscillations, to which the reader is referred for further details and extensive bibliography.

The paper is organized as follows. In Sec. II we discuss briefly the evidences for neutrino masses and mixings and introduce the notation for three-flavor oscillations. In Sec. III we discuss both hierarchical and non-hierarchical scenarios, and conclude that the latter are globally disfavored. In Sec. IV we identify a specific hierarchical framework that demands the "minimum sacrifice" of data. Its implications for current and future experiments are investigated in Sec. V. We draw the conclusions of our work in Sec. VI.

# II. NEUTRINO MASSES AND MIXINGS: EXPERIMENTAL EVIDENCES AND THREE-FLAVOR NOTATION

#### A. Evidences for neutrino mixing and oscillation

It is useful to start by making a distinction between evidences for neutrino mixing and for neutrino oscillation. We define "evidences for  $\nu$  mixing" those signals of flavor transitions, either direct (flavor appearance) or indirect (flavor disappearance), that imply nonzero mixing but do not provide a measurement of the oscillation wavelength. We then promote these basic signals to "evidences for  $\nu$  oscillation" only if, in addition, an effect related the periodicity of the flavor transition process (i.e., to the oscillation wavelength) is detected. In terms of neutrino events, evidences for mixing are simply established by "anomalous" measurements of total neutrino rates, while evidences for oscillation require, in addition, the more delicate observation of anomalous spectra of events as a function of either the neutrino path length L or the neutrino energy E.

The implications on the neutrino mass square difference  $\Delta m^2$  (assuming for the moment two neutrino families) are rather different in the two cases. An evidence for  $\nu$  mixing can only set a trivial lower bound on  $\Delta m^2$ , below which the oscillation length would largely overshoot the experimental baseline L and flavor transitions would not have time to develop.

An evidence for neutrino oscillations, instead, can give more detailed indications on  $\Delta m^2$  through the measured E or L spectra, since  $\Delta m^2$  appears either in the combination  $\Delta m^2 \times L/E$  (vacuum oscillations) or  $\Delta m^2/E$  (matter oscillations).

At present, there are three primary evidences for neutrino mixing: the overall deficit of the solar neutrino flux [1], the anomalous flavor ratio of total atmospheric rates [2], and the LSND event excess [3]. For the sake of brevity, they will be termed S (for solar), A (for atmospheric), and L (for LSND, laboratory), respectively. The following additional (and comparatively less established) observations may suggest genuine neutrino oscillation effects: (S') the solar neutrino deficit in different experiments [16] appears to depend significantly on the neutrino energy E (see [17] and references therein); (A') the atmospheric anomaly of multi-GeV neutrinos in Kamiokande seems to depend on the zenith angle (i.e., on the path length L) [18], although with uncertain statistical significance [12,19]; and (L') there is some evidence for a peak in the L/E spectrum of LSND events (see Fig. 32 in [3]).

Tables I and II list the above evidences for neutrino mixing and oscillation, respectively, together with their implications in terms of  $\Delta m^2$ . Notice that the evidences S, A, and L, are all compatible with large values of  $\Delta m^2$ , i.e. with fast (averaged) oscillations.<sup>1</sup> The evidence S' constrains  $\Delta m^2/\text{eV}^2$  to be either of  $\mathcal{O}(10^{-5})$  [10] or  $\mathcal{O}(10^{-10})$  [22], according to the specific solution called to explain the E-dependence of the solar  $\nu$  deficit [the Mikheyev-Smirnov-Wolfenstein (MSW) mechanism [23] or "just-so" vacuum oscillations [24], respectively]. The evidence A' requires  $\Delta m^2 \sim \mathcal{O}(10^{-2})$  eV<sup>2</sup> [18,13]. The weak evidence L' essentially excludes that the LSND detector position coincides with the "oscillation nodes," roughly corresponding to multiple integers of 4.3 eV<sup>2</sup> in  $\Delta m^2$  [3,15]. It should be noted that the evidences in Table II implicitly require the validity of the corresponding evidences in Table I, or, equivalently, that

$$X \text{ excluded} \Rightarrow X' \text{ excluded} \quad (X = S, A, \text{ or } L) .$$
 (1)

In the case of three-flavor oscillations, two independent mass square differences,  $\delta m^2$  and  $m^2$ , are involved. The  $\Delta m^2$  constraints in Tables I and II apply at least to one of them.

#### B. Three-family neutrino oscillation parameters

We adopt the standard parametrization [25,26] for the unitary mixing matrix  $U_{\alpha i}$  connecting the flavor eigenstates  $\nu_{\alpha} = \nu_{e,\mu,\tau}$  to the mass eigenstates  $\nu_i = \nu_{1,2,3}$  ( $\nu_{\alpha} = U_{\alpha i}\nu_i$ ):

$$U_{\alpha i} = \begin{pmatrix} c_{\omega} c_{\phi} & s_{\omega} c_{\phi} & s_{\phi} \\ -s_{\omega} c_{\psi} - c_{\omega} s_{\psi} s_{\phi} & c_{\omega} c_{\psi} - s_{\omega} s_{\psi} s_{\phi} & s_{\psi} c_{\phi} \\ s_{\omega} s_{\psi} - c_{\omega} c_{\psi} s_{\phi} & -c_{\omega} s_{\psi} - s_{\omega} c_{\psi} s_{\phi} & c_{\psi} c_{\phi} \end{pmatrix} , \tag{2}$$

where  $c = \cos$ ,  $s = \sin$ , and the mixing angles  $\omega$ ,  $\phi$ , and  $\psi$  range between 0 and  $\pi/2$ . Possible CP violation effects are neglected.

<sup>&</sup>lt;sup>1</sup>The recent data from the CCFR/NuTeV [20] experiment and the preliminary results from the NOMAD experiment [21] put, however, upper bounds on  $\Delta m^2$  in the same LSND channel ( $\sim 25$  and  $\sim 10 \text{ eV}^2$ , respectively).

Without loss of generality, we conventionally denote by  $\nu_1$ ,  $\nu_3$ , the two mass eigenstates separated by the largest mass gap. In particular,  $\nu_1$  is chosen to be the closest (in mass) to the intermediate state  $\nu_2$ . In terms of neutrino masses  $m_i$ , this choice is realized either with  $m_1 \leq m_2 \leq m_3$  or with  $m_3 \leq m_2 \leq m_1$ . We then define two independent mass square differences:

$$\delta m^2 = |m_2^2 - m_1^2| , \quad m^2 = |m_3^2 - m_2^2| , \qquad (3)$$

that, according to the above convention, obey the inequality  $\delta m^2 \leq m^2$ . A scenario with comparable square mass differences ( $\delta m^2 \sim m^2$ ) will be termed non-hierarchical. If  $\delta m^2$  is significantly smaller than  $m^2$ , the scenario will be termed hierarchical.

## III. FEATURES OF HIERARCHICAL $(\delta m^2 < m^2)$ AND NON-HIERARCHICAL $(\delta m^2 \sim m^2)$ SCENARIOS

In this section we classify all relevant three-flavor scenarios according to their spectrum of square mass differences  $\delta m^2$  and  $m^2$ , and comment briefly on their phenomenological implications. It will become evident that non-hierarchical spectra ( $\delta m^2 \sim m^2$ ) are a priori disfavored with respect to hierarchical spectra ( $\delta m^2 < m^2$ ).

For any neutrino experiment, there is a range of neutrino mass square difference where genuine oscillation effects are most relevant. For current solar, atmospheric, and laboratory (accelerator and reactor) experiments, these ranges happen to be roughly decoupled as  $[0, 10^{-3.5}], [10^{-3.5}, 10^{-1.5}], \text{ and } [10^{-1.5}, \infty], \text{ respectively (in units of eV}^2) [10-15].$  Therefore, it is useful to introduce the following shorthand notation for these indicative  $\Delta m^2$  ranges:

$$\Delta m^2 \sim \Delta m_{\text{sun}}^2 \iff \Delta m^2 \lesssim 10^{-3.5} \text{ eV}^2$$
, (4)

$$\Delta m^{2} \sim \Delta m_{\text{sun}}^{2} \iff \Delta m^{2} \lesssim 10^{-3.5} \text{ eV}^{2} ,$$

$$\Delta m^{2} \sim \Delta m_{\text{atm}}^{2} \iff 10^{-3.5} \lesssim \Delta m^{2} \lesssim 10^{-1.5} \text{ eV}^{2} ,$$

$$\Delta m^{2} \sim \Delta m_{\text{lab}}^{2} \iff \Delta m^{2} \gtrsim 10^{-1.5} \text{ eV}^{2} ,$$

$$(5)$$

$$\Delta m^{2} \sim \Delta m_{\text{lab}}^{2} \iff \Delta m^{2} \gtrsim 10^{-1.5} \text{ eV}^{2} ,$$

$$(6)$$

$$\Delta m^2 \sim \Delta m_{\rm lab}^2 \iff \Delta m^2 \gtrsim 10^{-1.5} \text{ eV}^2$$
, (6)

where  $\Delta m^2$  denotes either  $\delta m^2$  or  $m^2$ .

Table III shows a classification of the  $(\delta m^2, m^2)$  spectra in terms of the above ranges. Six scenarios can be identified. The first three are hierarchical, the last three are nonhierarchical. None of the six cases can fit all the evidences for neutrino mixing (S, A, L in Table I) and for neutrino oscillations (S', A', L' in Table II), as emphasized in the last column of Table III that we now discuss.

In the first three (hierarchical) cases,  $\delta m^2$  and  $m^2$  are chosen in two different ranges, so as to solve two out of the three "neutrino problems" posed by the solar deficit, the atmospheric anomaly, and the LSND event excess. In the first scenario, one chooses to fit the solar and the laboratory neutrino data. However, this case is not compatible with A', since  $\delta m^2$  and  $m^2$  are, respectively, too small or too large to produce a zenith-angle dependence of the atmospheric anomaly. The second scenario can provide a good fit to solar and atmospheric data, but is not compatible with the evidence L, since  $\delta m^2$  and  $m^2$  are below the LSND sensitivity. The third scenario can fit well both atmospheric and laboratory data. However, due to the assumption of large values for  $\delta m^2$  and  $m^2$ , the solar neutrino deficit is predicted to be energy-independent and the evidence S' must be abandoned.

In the last three, non-hierarchical scenarios, both  $\delta m^2$  and  $m^2$  are assumed to be in the same range, thus "oversolving" one of the three neutrino problems, at the expenses of the other two. In particular, the 4th and 5th scenarios in Table III are not compatible with L, for the same reason as for the 2nd scenario. In addition, in case 4 the evidence A must be abandoned,  $\delta m^2$  and  $m^2$  being too small to produce observable effects for atmospheric neutrinos. In case 5, S' must be abandoned for the same reason as for case 3. The reader is referred to Refs. [26] and [27] for studies of subcases of the 4th and 5th scenario, respectively. The 6th (and last) scenario of Table III is incompatible with S' and A', since both  $\delta m^2$  and  $m^2$  are too large to produce E-dependent (L-dependent) effects for solar (atmospheric) neutrinos. To our knowledge, there is no recent, post-LSND paper addressing case 6.

Since our goal is to identify the three-flavor scenario that requires the "minimum sacrifice" of data, we will not further consider the non-hierarchical scenarios 4, 5, and 6 listed in Table III. The hierarchical scenarios 1, 2, and 3 will be instead investigated in detail in the next section.

#### IV. GRADING HIERARCHICAL CASES

The analyses of the hierarchical cases (1, 2, 3 in Table III) are greatly simplified if the calculations are performed at zeroth order in the ratio  $\delta m^2/m^2$  [28]. This is usually a good approximation, provided that the relevant values of  $\delta m^2$  and  $m^2$  are separated by at least an order of magnitude (see [28] and references therein). CP violation effects vanish as  $\delta m^2/m^2 \to 0$ , and thus can also be neglected. Within this approximation (sometimes called "one mass scale dominance"), we set out to analyze in detail the three hierarchical scenarios, after a brief discussion of the neutrino oscillation probabilities.

#### A. Oscillation probabilities

Table IV reports the functional form of the three-flavor neutrino oscillation probabilities  $P^{\alpha\beta} = P(\nu_{\alpha} \to \nu_{\beta})$  for solar, atmospheric, and laboratory neutrinos—at zeroth order in  $\delta m^2/m^2$ —for each of the three hierarchical scenarios 1, 2, and 3. In each specific case, the probability depends only on a subset of the full  $3\nu$  parameter space  $(\delta m^2, m^2, U_{\alpha i})$ .

For solar neutrinos,  $P_{\text{sun}}^{ee}$  can take two functional forms,  $P_{\text{MSW}}^{ee}$  or  $P_{\text{vac}}^{ee}$ , according to the specific solution adopted for the solar neutrino problem (MSW or vacuum oscillations, respectively). The explicit  $3\nu$  expressions of  $P_{\text{MSW}}^{ee}$  and  $P_{\text{vac}}^{ee}$  can be found, for instance, in [10] and [11], respectively. In both cases (MSW and vacuum) and for both the first and the second scenario,  $P_{\text{sun}}^{ee}$  depends only on the parameters  $(\delta m^2, U_{e1}, U_{e2}, U_{e3})$ , which are further constrained by unitarity. In the limit of small  $U_{e3}$ , the expression of  $P_{\text{sun}}^{ee}$  takes a more familiar two-family form. In the limit of large  $\delta m^2$  (scenario 3) both  $P_{\text{MSW}}^{ee}$  and  $P_{\text{vac}}^{ee}$  assume the simple form given in the seventh row of Table IV. Useful graphical representations of the solar  $\nu$  parameter space spanned by  $(U_{e1}, U_{e2}, U_{e3})$  [or, equivalently, by  $(\omega, \phi)$ ] at fixed  $\delta m^2$  were introduced in [10]. In particular, we will make use of the  $(\tan^2 \omega, \tan^2 \phi)$  bilogarithmic chart [10].

For atmospheric neutrinos, the flavor oscillation probabilities take a very simple form, as far as MSW effects in the Earth are ignored. The inclusion of matter effects is not decisive

for a qualitative understanding and, in any case, it does not require additional mass-mixing parameters in the expression of P, besides those listed in Table IV [13]. In the 2nd scenario, the atmospheric  $\nu$  parameter space is  $(m^2, U_{e3}, U_{\mu 3}, U_{\tau 3})$ . A useful graphical representation at fixed  $m^2$  is represented by the  $(\tan^2 \psi, \tan^2 \phi)$  bilogarithmic chart [13,14], which can also be used for scenario 1. Finally, in the third (hierarchical) scenario,  $P_{\rm atm}$  depends on the whole mixing matrix (besides  $\delta m^2$ ) and no simple graphical representation of the parameter space can be given.

For laboratory (accelerator and reactor) neutrinos, the oscillation probabilities in Table IV are even simpler than for atmospheric  $\nu$ 's, due to the absence of matter effects. The second scenario excludes any oscillation effect in laboratory neutrino beams, since both  $\delta m^2$  and  $m^2$  are small by assumption. Notice that the laboratory  $\nu$  parameter space  $(m^2, U_{e3}, U_{\mu 3}, U_{\tau 3})$  can be charted by the variables  $(\tan^2 \psi, \tan^2 \phi)$  at fixed  $m^2$ , as shown in [14,15].

**B. Scenario 1:** 
$$(\delta m^2, m^2) \sim (\Delta m_{\text{sun}}^2, \Delta m_{\text{lab}}^2)$$

In this scenario, the parameter space of laboratory (accelerator and reactor) neutrino oscillations is spanned by  $m^2$  and  $U_{\alpha 3}^2$  (see Table IV) or, equivalently, by  $m^2$ ,  $\phi$ , and  $\psi$  [see Eq. (2)]. For this case, the constraints provided by all laboratory data, including LSND, have been detailedly worked out in [15]. In particular, we refer to Fig. 4 of [15], which shows the global bounds in the  $(\tan^2 \psi, \tan^2 \phi)$  plane for representative values of  $m^2$ . These bounds identify two possible solutions at 90% C.L., one at "large  $\phi$ " and the other at "small  $\phi$ ." The "large  $\phi$ " solution corresponds to  $U_{e3} \sim 1$ , that is, to  $\nu_e$  almost coincident with the mass eigenstate  $\nu_3$ . In this case, the deficit of solar neutrinos would be of order  $(1-U_{e3}^2)^2$  and thus negligible [10], in contrast with the evidence S. The "small  $\phi$ " solution is also characterized by large values of  $\psi$  and thus it corresponds to a  $U_{\mu 3} \sim 1$ , i.e., to  $\nu_{\mu}$  almost coincident with the mass eigenstate  $\nu_3$ . In this case, the remaining flavor states  $(\nu_e, \nu_\tau)$  have to be mixed prevalently with the mass eigenstates  $(\nu_1, \nu_2)$ , implying that solar neutrino oscillations are almost pure  $\nu_e \leftrightarrow \nu_\tau$ .

The above considerations imply that in the scenario 1 all the laboratory results (including the LSND evidences L and L') and all the solar neutrino data (evidences S and S') can be reconciled by combining the "small  $\phi$ " solution of laboratory  $\nu$  fits [15] with almost pure  $\nu_e \to \nu_\tau$  oscillations for solar neutrinos. The  $\nu_e \to \nu_\tau$  oscillations can be assumed either of the MSW type [23] or of the vacuum oscillation type [24]. In the MSW case, the bounds in the solar neutrino parameter space  $(\delta m^2, \omega, \phi)$  have been explicitly worked out in [10]. In particular, Fig. 12 in [10] shows that in the limit of large  $\phi$  no solution is allowed, while in the limit of small  $\phi$  one recovers the familiar "small  $\omega$ " and "large  $\omega$ " solutions usually found in two-family MSW fits.

It remains to be seen whether the atmospheric data can also be fitted in this scenario. We have already observed in Table III that one cannot fit the evidence A' in this case. Indeed, the global three-flavor fits to the atmospheric  $\nu$  data (including the evidences A and A') [13] and to the laboratory  $\nu$  data [15] favor two different, incompatible ranges for  $m^2$ . However, it has been noted by Cardall and Fuller [5] that the sole exclusion of the evidence A' allows the laboratory and the atmospheric data to be (marginally) reconciled at  $m^2 \sim 0.4$  eV<sup>2</sup>. It

must be said that the evidence A' is somewhat uncertain. Its statistical significance might be smaller [12,19] than the value originally quoted by the Kamiokande collaboration [18]. Moreover, A' is not confirmed by a recent reanalysis of older data from the IMB experiment [29]. The SuperKamiokande experiment [30] is expected to clarify soon this issue.

Motivated by the semiquantitative results of [5] we have repeated a global fit to all atmospheric data as in [13], but with unbinned multi-GeV Kamiokande data, so as to integrate out their zenith-angle dependence (evidence A'). The results of this new fit are reported in Fig. 1. Figure 1 shows, in the  $(\tan^2 \psi, \tan^2 \phi)$  plane and for the representative value  $m^2 = 0.45 \text{ eV}^2$ , the regions allowed at 90% C.L. by fits to all laboratory data (dashed line) and to all sub-GeV and unbinned multi-GeV atmospheric data (dotted line). It can be seen that these two regions overlap, although marginally, at  $(\tan^2 \psi, \tan^2 \phi) \sim (7, 0.0035)$ . Therefore, it makes sense to perform a combined fit. The resulting solution is shown as a solid contour in Fig. 1. Its area is larger than the simple intersection of the previous two regions, as is the case for the combination of data that are marginally compatible; therefore, its shape must be taken with caution. Actually, this solution appears only in the narrow range  $0.3 \lesssim m^2 \lesssim 0.5 \text{ eV}^2$ , as also noticed in [5].

Figure 2 represents a concise summary of the global fit(s) to neutrino oscillation data (excluding A') in the three-flavor scenario 1. The  $(\tan^2 \psi, \tan^2 \phi)$  plane on the left (which reports a schematic reduction of Fig. 1) is basically the parameter space of the neutrino state  $\nu_3$  [14,15]. As already noticed, the "terrestrial" (laboratory and atmospheric) data impose  $(\tan^2 \psi, \tan^2 \phi) \sim (7, 0.0035)$ . This solution survives with similar characteristics in the range  $0.3 \lesssim m^2 \lesssim 0.5 \text{ eV}^2$ . The  $(\tan^2 \omega, \tan^2 \phi)$  plane on the right of Fig. 2 maps the parameter space of solar  $\nu_e$ 's. For the small value of  $\phi$  fixed by the terrestrial  $\nu$  fit, solar neutrino oscillations are almost pure  $\nu_e \leftrightarrow \nu_\tau$ . Three solutions are possible: (1a) small angle MSW; (1b) large angle MSW; and (1c) vacuum oscillations. The mass and mixing parameters corresponding to these three possible solutions are reported in Table V. The given  $\tan^2 \nu$  values may vary within a factor of about two, as reminded by the "thickness" of the black dots in Fig. 2. Finally, the flavor components of  $\nu_3$  and the mass components of  $\nu_e$  are explicitly worked out at the bottom of Fig. 2, for the mixing values reported in Table V.

In conclusion, terrestrial and solar neutrino data can all be fitted within the three-flavor scenario 1, with the only exclusion of the zenith-angle dependence of the atmospheric  $\nu$  anomaly (evidence A'). The resulting constraints in the space  $(\delta m^2, m^2, \omega, \phi, \psi)$  are rather stringent for each of the three possible solutions corresponding to different solar  $\nu$  fits. As we will see, the two remaining hierarchical scenarios 2 and 3 demand more drastic exclusions of data. In this sense, the scenario 1 requires the "minimum sacrifice." Its implications will be studied in Sec. V.

C. Scenario 2: 
$$(\delta m^2, m^2) \sim (\Delta m_{\rm sun}^2, \Delta m_{\rm atm}^2)$$

This case requires the sacrifice of the whole LSND data set (evidence L) as noted in Table III and related comments. In view of the fact that new, independent LSND data from pion decay in flight [31] have recently confirmed the existing LSND data from muon decay at rest [3], this appears a more drastic rejection than the exclusion of A' in the previously analyzed scenario 1.

In scenario 2, one has to combine the negative laboratory oscillation searches with the atmospheric and solar neutrino data. The complete three-flavor analysis of atmospheric neutrino data performed in [13] applies to this case. The bounds on the  $(m^2, \psi, \phi)$  parameter space are given in Fig. 7 of Ref. [13] for atmospheric data only, and in Fig. 11 of the same paper for atmospheric and laboratory data (without LSND). Concerning the MSW solution to the solar neutrino problem, the  $(\delta m^2, \omega, \phi)$  bounds appropriate to this scenario can be read from Fig. 12 in [10].<sup>2</sup> The match between solar and terrestrial bounds requires that the common parameter  $\phi$  assume the same value in both fits. This exercise is made easier by the fact that the panels of Fig. 12 in [10] and the panels of Figs. 7 and 11 in [13] exhibit purposely the same values of  $\tan^2 \phi$  on the y-axis.

The so-called "threefold maximal mixing" framework of Harrison, Perkins, and Scott [9] is a subcase of this scenario. It corresponds to  $|U_{\alpha i}|^2 = 1/3$ , i.e., to  $(\tan^2 \omega, \tan^2 \phi, \tan^2 \psi) = (1, 1/2, 1)$  (at any value of  $\delta m^2$ ,  $m^2$ ). The point  $(\tan^2 \phi, \tan^2 \psi) = (1/2, 1)$  is allowed by terrestrial  $\nu$  data, provided that  $m^2$  is below the sensitivity of the established laboratory experiments (that do not allow large neutrino mixing) [14]. However, the point  $(\tan^2 \omega, \tan^2 \phi) = (1, 1/2)$  is excluded by the MSW analysis of solar  $\nu$  data at more than 99% C.L. [10]. The same point might be instead allowed by the vacuum oscillation solution of solar  $\nu$  data, as suggested in [9], although a detailed three-flavor analysis of this situation has not been performed yet.

**D. Scenario 3:** 
$$(\delta m^2, m^2) \sim (\Delta m_{\rm atm}^2, \Delta m_{\rm lab}^2)$$

This scenario has been recently studied in [6,7] and, in particular, by Acker and Pakvasa in [8]. It is particularly appealing to researchers of laboratory neutrino oscillations, since  $\Delta m_{\rm lab}^2$  represents the range explorable by present and future short baseline experiments, and  $\Delta m_{\rm atm}^2$  covers the range explorable by future long baseline experiments. At first sight, this scenario seems to require only the exclusion of the evidence S' (see Table III). However, a more detailed investigation shows that additional sacrifices of data are necessary.

Let us consider first the chain of constraints imposed by the negative oscillation searches at accelerators and reactors in the parameter space  $(m^2, U_{\alpha 3}) \equiv (m^2, \phi, \psi)$ , as spanned by  $\nu_3$  [14]. The LSND data will be reintroduced at the end. The negative laboratory searches in all channels constrain  $\nu_3$  to be close to one of the mass eigenstates, in order to suppress the (unobserved) oscillation phenomena. In Table VI, the three possible cases  $\langle \nu_3 | \nu_\alpha \rangle \sim 1$  with  $\alpha = e, \mu$ , or  $\tau$ , are labeled 3a, 3b, and 3c, respectively. For each case, the resulting (approximate) structure of the mixing matrix is given in the third column, where the parameters a, b, and c are a priori unconstrained. The fourth column in Table VI gives the expression of the solar neutrino survival probability, as derived from Table IV for the scenario 3 and its subcases 3a, 3b, and 3c. Notice that for  $\langle \nu_3 | \nu_e \rangle \sim 1$  (case 3a) the states  $\nu_1$  and  $\nu_2$  must be essentially a mixture of  $\nu_\mu$  and  $\nu_\tau$ . Therefore, in case 3a the atmospheric neutrino oscillations are almost pure  $\nu_\mu \leftrightarrow \nu_\tau$ , with an effective mixing amplitude  $\sin^2 \theta_{\rm eff}^{\rm eff}$ 

<sup>&</sup>lt;sup>2</sup>An analogous, detailed  $3\nu$  analysis is still lacking for the vacuum oscillation solution to the solar neutrino problem. See, however, [32] for a recent  $3\nu$  fit.

equal to 4a(1-a), as given in the last column of Table VI. Similar considerations apply to cases 3b and 3c. In other words, atmospheric neutrino oscillations are governed in each case by the only nontrivial  $2 \times 2$  submatrix of the mixing matrix. We remark that the properties listed in the third, fourth and fifth column of Table VI follow solely from the assumption in the first column of the same Table, i.e. from the negative results of laboratory oscillation searches.

From Table VI it follows that the case 3a is compatible with the atmospheric evidences A and A', fitted with almost pure  $\nu_{\mu} \leftrightarrow \nu_{\tau}$  oscillations. However, this subcase predicts  $P_{\rm sun}^{ee} \sim 1$  and thus no neutrino deficit. Conversely, in case 3b one can obtain a solar neutrino deficit by tuning the free parameter b, but then aggravates (instead of solving) the atmospheric neutrino anomaly through  $\nu_e \leftrightarrow \nu_{\tau}$  oscillations.

Only the case 3c seems to survive, since with a judicious choice of the free parameter c (Table III) one can obtain both a significant deficit of solar neutrinos and a solution to the atmospheric anomaly through  $\nu_e \leftrightarrow \nu_\mu$  oscillations. (It is precisely this scenario that was studied in [8].) As far as the LSND data are excluded, it seems to provide a reasonable fit to all data (excluding, of course, the evidence S'). However, as shown in [15], the inclusion of the LSND results in the fit to laboratory  $\nu$  data strongly disfavors the situation  $\langle \nu_3 | \nu_\tau \rangle \sim 1$ , i.e. the case 3c. In fact, the two possible solutions found at 90% C.L. in [15] at any given  $m^2$  (see also Fig. 1 of this work) correspond to cases 3a and 3b, respectively. The semiquantitative analyses in [6–8] and [33] found an allowed solution corresponding to case 3c only by "stretching" all the uncertainties of the laboratory data (including LSND) to their 90% C.L. limits.<sup>3</sup> However, the overall C.L. of this contrived situation certainly exceeds 90%. Indeed, a proper statistical analysis excludes the case 3c at  $\sim$  99% C.L. [15]. A similar conclusion about the case 3c was independently reached in [34].

In conclusion, the scenario 3 is incompatible not only with S', but also with other evidences for neutrino oscillations, depending on the specific subcase studied (3a, 3b, or 3c in Table VI). The claim that in this framework "three neutrino flavors are enough" to fit the world neutrino data [8] is not substantiated by a quantitative analysis—one has to discard at least a primary evidence for mixing (S, A, or L) in order to achieve a reasonable fit. A summary of the data not compatible with scenario 3 is given in Table VII.

#### V. IMPLICATIONS OF THE "MINIMUM SACRIFICE" SCENARIO

In this section we discuss the implications of the scenario 1 that, at present, emerges as the three-flavor framework consistent with the largest amount of neutrino data. Only the zenith-angle dependence of the multi-GeV Kamiokande data is incompatible with this scenario. Therefore, an immediate "falsification" of this framework could be provided by the high-statistics SuperKamiokande experiment, should it confirm the zenith-angle dependence of the atmospheric  $\nu$  anomaly found in kamiokande [18]. Preliminary results from

<sup>&</sup>lt;sup>3</sup>In our notation, Ref. [8,33] studied the case 3c, Ref. [6] the cases 3a and 3c, and Ref. [7] the cases 3a, 3b, and 3c.

SuperKamiokande [30] confirm the anomaly of the *total* rates, but do not provide yet any decisive indication on the zenith-angle spectrum.

Assuming that the scenario 1 survives the SuperKamiokande test, which are its implications on solar and laboratory neutrino oscillation searches? As discussed in Sec. IV B, solar neutrino oscillations are predicted to be almost pure  $\nu_e \leftrightarrow \nu_\tau$  in this case. Unfortunately, since solar neutrino experiments do not distinguish  $\nu_\mu$ 's from  $\nu_\tau$ 's in solar neutrino experiments, we do not expect important indications on this scenario from the new-generation solar  $\nu$  detectors SuperKamiokande [30] or Sudbury Neutrino Observatory (SNO) [35].

Short-baseline laboratory oscillations should, instead, give important information. Figure 3 shows the solution corresponding to scenario 1 (thick, solid line), together with the regions of the mixing parameter space that will be probed by the KARMEN experiment [36] (exploring the same LSND channel  $\bar{\nu}_{\mu} \leftrightarrow \bar{\nu}_{e}$ ) at the end of 1999, by the CERN experiments CHORUS [37] and NOMAD [38] ( $\nu_{\mu} \leftrightarrow \nu_{\tau}$ ) in four years of data taking, and by the proposed  $\nu_{\mu} \leftrightarrow \nu_{\tau}$  experiments COSMOS [39] at Fermilab and TENOR/NAUSICAA [40] or TOSCA [41] at CERN. It can be seen that these experiments can probe either a fraction or all of the proposed solution. It is particularly interesting to note that, although this solution is governed by the results of a  $\bar{\nu}_{\mu} \leftrightarrow \bar{\nu}_{e}$  experiment (LSND), it can be completely covered by sensitive  $\nu_{\mu} \leftrightarrow \nu_{\tau}$  experiments (COSMOS, TOSCA, or TENOR/NAUSICAA). This feature would have gone unnoticed in a two-flavor analysis.

Concerning long-baseline experiments, the current reactor projects Chooz [42] and Palo Verde [43] have not sufficient sensitivity in mixing to probe the solution in Fig. 3, and, in general, the LSND signal [15]. In accelerator experiments, the solution of Fig. 3 would induce oscillations with a wavelength much smaller than the (long) baseline. The finite energy bandwidth of the beam and of the detector would then smear out the oscillation pattern, giving rise to evidences of mixing at best. This would, in a sense, defeat main purpose and hope of long-baseline experiments.

#### VI. CONCLUSIONS

We have analyzed how well various possible three-flavor scenarios can fit the world neutrino data from oscillation searches in solar and terrestrial (atmospheric and laboratory) experiments. In any case some data must be "sacrificed." Scenarios with no hierarchy in the spectrum of neutrino mass differences are shown to be a priori disfavored. A specific hierarchical framework emerges naturally as the "minimum sacrifice" fit to the data. The characteristics and the phenomenological consequences of this scenario have been investigated. If this scenario survives the stringent test of the SuperKamiokande atmospheric measurements, then future short-baseline searches at accelerator facilities will play a decisive role in its (dis)confirmation.

#### ACKNOWLEDGMENTS

One of us (G.L.F.) thanks the organizers of the Workshop on Fixed Target Physics at the Fermilab Main Injector, Fermilab, Batavia IL, where preliminary results of this work were presented.

TABLES

TABLE I. Evidences for neutrino mixing and their implications on  $\Delta m^2$ .

Primary evidence (for $\nu$ mixing)	Symbol	Implications for $\Delta m^2$
Solar $\nu_e$ deficit	S	$\Delta m^2 \gtrsim 10^{-11} \text{ eV}^2$
Atmospheric $\nu_{\mu}/\nu_{e}$ anomaly	A	$\Delta m^2 \gtrsim 10^{-4} \text{ eV}^2$
LSND $\bar{\nu}_e$ signal	${f L}$	$\Delta m^2 \gtrsim 10^{-1} \ \mathrm{eV^2}$

TABLE II. Evidences for neutrino oscillations and their implications on  $\Delta m^2$ .

Additional evidence (for $\nu$ oscillation)	Symbol	Implications for $\Delta m^2$
$E$ -dependence of solar $\nu$ deficit	S'	$\Delta m^2 \sim 10^{-5} \text{ eV}^2 \text{ (MSW) or}$ $\Delta m^2 \sim 10^{-10} \text{ eV}^2 \text{ (vacuum)}$
$L$ -dependence of atmospheric $\nu$ anomaly	$\mathrm{A}'$	$\Delta m^2 \sim 10^{-2} \text{ eV}^2$
$(L/E)$ -dependence of LSND $\nu$ signal	$\mathrm{L}'$	$\Delta m^2 \not\simeq n \times 4.3 \text{ eV}^2 \ (n = 1, 2, 3, \ldots)$

TABLE III. Classification of  $3\nu$  scenarios according to their spectrum of square mass differences  $(\delta m^2, m^2)$ , as compared with the phenomenologically relevant  $\Delta m^2$  ranges. The first three scenarios are "hierarchical"  $(\delta m^2 < m^2)$ , the last three "non-hierarchical"  $(\delta m^2 \sim m^2)$ . The last column shows the (minimum) set of evidences incompatible with the various scenarios.

	Ranges of $\nu$ square mass difference (eV <sup>2</sup> )			
	$\Delta m_{ m sun}^2$	$\Delta m^2_{ m atm}$	$\Delta m_{ m lab}^2$	Evidences to be
Scenario	$\Delta m_{\rm sun}^2 \lesssim 10^{-3.5}$	$\sim 10^{-3.5} - 10^{-1.5}$	$\gtrsim 10^{-1.5}$	discarded (at least)
1	$\delta m^2$		$m^2$	A'
2	$\delta m^2$	$m^2$		${ m L}$
3		$\delta m^2$	$m^2$	S'
4	$\delta m^2,  m^2$			L and A
5		$\delta m^2,m^2$		L and $S'$
6			$\delta m^2,m^2$	A' and $S'$

TABLE IV. Functional form of the oscillation probabilities for solar, atmospheric, and laboratory neutrino beams, in each of the hierarchical scenarios 1, 2, and 3.

Scenario	P	Parameters	Functional form of the oscillation probability <sup>a</sup>
	$P_{\sup}^{ee}$	$(\delta m^2, U_{ei})$	$P_{\mathrm{MSW}}^{ee}(\delta m^2, U_{ei})$ or $P_{\mathrm{vac}}^{ee}(\delta m^2, U_{ei})$
1	$P_{ m atm}^{lphaeta}$	$(U_{\alpha 3},U_{\beta 3})$	$\delta_{\alpha\beta} - 2U_{\alpha3}U_{\beta3}(\delta_{\alpha\beta} - U_{\alpha3}U_{\beta3}) + matter\ effects$
	$P_{\text{atm}}^{\alpha\beta} \\ P_{\text{lab}}^{\alpha\beta}$	$(m^2, U_{\alpha 3}, U_{\beta 3})$	$\delta_{\alpha\beta} - 4U_{\alpha3}U_{\beta3}(\delta_{\alpha\beta} - U_{\alpha3}U_{\beta3})\sin^2(1.27m^2L/E)$
	$P_{\sup}^{ee}$	$(\delta m^2, U_{ei})$	$P_{\text{MSW}}^{ee}(\delta m^2, U_{ei})$ or $P_{\text{vac}}^{ee}(\delta m^2, U_{ei})$
2	$P_{ m atm}^{lphaeta}$	$(m^2, U_{\alpha 3}, U_{\beta 3})$	$\delta_{\alpha\beta} - 4U_{\alpha3}U_{\beta3}(\delta_{\alpha\beta} - U_{\alpha3}U_{\beta3})\sin^2(1.27m^2L/E) + matter\ effects$
	$P_{ ext{sun}}^{ee}$ $P_{ ext{atm}}^{lphaeta}$ $P_{ ext{lab}}^{lphaeta}$	_	$\delta_{lphaeta}$
	$P_{\rm sun}^{ee}$	$(U_{ei})$	$1 - 2(U_{e1}^2 U_{e2}^2 + U_{e2}^2 U_{e3}^2 + U_{e3}^2 U_{e1}^2)$
3	$P_{ m atm}^{lphaeta}$	$(\delta m^2, U_{\alpha i}, U_{\beta i})$	$\delta_{\alpha\beta} - 2U_{\alpha3}U_{\beta3}(\delta_{\alpha\beta} - U_{\alpha3}U_{\beta3}) - 4U_{\alpha1}U_{\alpha2}U_{\beta1}U_{\beta2}\sin^2(1.27\delta m^2L/E) + matter\ effects$
	$P_{\rm atm}^{\alpha\beta} \\ P_{\rm lab}^{\alpha\beta}$	$(m^2, U_{\alpha 3}, U_{\beta 3})$	$\delta_{\alpha\beta} - 4U_{\alpha3}U_{\beta3}(\delta_{\alpha\beta} - U_{\alpha3}U_{\beta3})\sin^2(1.27m^2L/E)$

 $<sup>{\</sup>rm ^aUnits:}\ [\delta m^2],\,[m^2]={\rm eV^2},\,[L]={\rm m},\,[E]={\rm MeV}.$ 

TABLE V. Scenario 1: Summary of the neutrino mass-mixing parameters for the three possible subcases 1a, 1b, and 1c. Mixings are determined up to a factor of about two.

Scenario	$m^2 (eV^2)$	$\tan^2 \psi$	$\tan^2 \phi$	Solar neutrino solution	$\delta m^2 \; ({\rm eV^2})$	$\tan^2 \omega$
1a	$\sim 0.30.5$	$\sim 7$	$\sim 0.0035$	MSW, small $\omega$	$\sim 0.4 1 \times 10^{-5}$	$\sim 0.0015$
1b	$\sim 0.30.5$	$\sim 7$	$\sim 0.0035$	MSW, large $\omega$	$\sim 0.6 9 \times 10^{-5}$	$\sim 0.25$
1c	$\sim 0.3  0.5$	$\sim 7$	$\sim 0.0035$	vacuum oscillation	$\sim 0.5 1 \times 10^{-10}$	$\sim 1$

TABLE VI. Scenario 3: Implications of negative oscillation searches for solar and atmospheric neutrino oscillations. See the text for details.

Scenario	$\nu_3$ from negative lab. searches	Approximate structure of $U_{\alpha i}^2$	Implications for solar neutrinos	Implications for atmospheric neutrinos
3a	$\langle \nu_3   \nu_e \rangle \sim 1$	$ \left(\begin{array}{cccc} 0 & 0 & 1 \\ 1 - a & a & 0 \\ a & 1 - a & 0 \end{array}\right) $	$P_{ m sun}^{ee} \sim 1$	$\sim (\nu_{\mu},  \nu_{\tau}) \text{ oscillations},$ $\sin^2 2\theta_{\mu\tau}^{\text{eff}} \sim 4a(1-a)$
3b	$\langle  u_3    u_\mu  angle \sim 1$	$ \left(\begin{array}{ccc} 1 - b & b & 0 \\ 0 & 0 & 1 \\ b & 1 - b & 0 \end{array}\right) $	$P_{\rm sun}^{ee} \sim 1 - 2b(1-b)$	$\sim (\nu_e,  \nu_{\tau}) \text{ oscillations},$ $\sin^2 2\theta_{e\tau}^{\text{eff}} \sim 4b(1-b)$
3c	$\langle \nu_3   \nu_{\tau} \rangle \sim 1$	$ \left(\begin{array}{ccc} 1 - c & c & 0 \\ c & 1 - c & 0 \\ 0 & 0 & 1 \end{array}\right) $	$P_{\rm sun}^{ee} \sim 1 - 2c(1-c)$	$\sim (\nu_e,  \nu_\mu)$ oscillations, $\sin^2 2\theta_{e\mu}^{\text{eff}} \sim 4c(1-c)$

TABLE VII. Scenario 3: Summary of the evidences to be discarded in each of the three subcases 3a, 3b, and 3c.

	Incompatible
Scenario	evidence(s)
3a	S
3b	S', A
3c	S', L

## REFERENCES

- [1] J. N. Bahcall, *Neutrino Astrophysics* (Cambridge University Press, Cambridge, England, 1989); J. N. Bahcall and M. H. Pinsonneault, in *Neutrino '96*, 17th International Conference on Neutrino Physics and Astrophysics, Helsinki, Finland, 1996, to appear in the Proceedings (hep-ph/9610542).
- [2] A. Suzuki, in the Proceedings of the 7th International Conference on Neutrino Telescopes, Venice, Italy, 1996, edited by M. Baldo Ceolin (University of Padova, Italy, 1996), p. 263; T. K. Gaisser, in Neutrino '96 [1] (hep-ph/9611301).
- [3] LSND Collaboration, C. Athanassopoulos et al., Phys. Rev. C 54, 2658 (1996); Phys. Rev. Lett. 77, 3082 (1996).
- [4] A. Yu. Smirnov, in *ICHEP '96*, 28th International Conference on High-Energy Physics, Warsaw, Poland, 1996, to appear in the Proceedings (hep-ph/9611465).
- [5] C. Y. Cardall and G. M. Fuller, Phys. Rev. D 53, 4421 (1996).
- [6] H. Minakata, Phys. Rev. D 52, 6630 (1995).
- [7] S. Goswami, K. Kar, and A. Raychaudhuri, Int. J. Mod. Phys. A 12, 781 (1997).
- [8] A. Acker and S. Pakvasa, Phys. Lett. B 397, 209 (1997).
- [9] P. F. Harrison, D. H. Perkins, and W. G. Scott, Phys. Lett. B 349, 137 (1995); 396, 186 (1997).
- [10] G. L. Fogli, E. Lisi, and D. Montanino, Phys. Rev. D 54, 2048 (1996).
- [11] B. Faïd, G. L. Fogli, E. Lisi, and D. Montanino, Phys. Rev. D 55, 1353 (1997).
- [12] G. L. Fogli and E. Lisi, Phys. Rev. D **52**, 2775 (1995).
- [13] G. L. Fogli, E. Lisi, D. Montanino, and G. Scioscia, Phys. Rev. D 55, 4385 (1997).
- [14] G. L. Fogli, E. Lisi, and G. Scioscia, Phys. Rev. D 52, 5334 (1995).
- [15] G. L. Fogli, E. Lisi, and G. Scioscia, University of Bari Report No. BARI-TH-259-97, hep-ph/9702298, to appear in Phys. Rev. D.
- [16] See talks by K. Lande (Homestake Collaboration), Y. Suzuki (Kamiokande Collaboration), T. Kirsten (GALLEX Collaboration), and V. Gavrin (SAGE Collaboration) in *Neutrino '96* [1].
- [17] P. I. Krastev and S. T. Petcov, Phys. Lett. B **395**, 69 (1997).
- [18] Kamiokande Collaboration, Y. Fukuda et al., Phys. Lett. B 335, 237 (1994).
- [19] D. Saltzberg, Phys. Lett. B **355**, 499 (1995).
- [20] CCFR/NuTeV Collaboration, A. Romosan et al., Phys. Rev. Lett. 78, 2912 (1997).
- [21] L. DiLella, private communication.
- [22] P. I. Krastev and S. T. Petcov, Phys. Rev. D **53**, 1665 (1996).
- [23] L. Wolfenstein, Phys. Rev. D 17, 2369 (1978); S. P. Mikheyev and A. Yu. Smirnov, Yad.
   Fiz. 42, 1441 (1985) [Sov. J. Nucl. Phys. 42, 913 (1985)]; Nuovo Cim. C 9, 17 (1986).
- [24] S. L. Glashow and L. M. Krauss, Phys. Lett. B **190**, 199 (1987).
- [25] Review of Particle Physics, R. M. Barnett et al., Phys. Rev. D 54, 1 (1996).
- [26] T. K. Kuo and J. Pantaleone, Rev. Mod. Phys. 61, 937 (1989).
- [27] O. Yasuda, Tokyo Metropolitan University Report No. TMUP-HEL-9603, hep-ph/9602342 (unpublished).
- [28] G. L. Fogli, E. Lisi, and D. Montanino, Phys. Rev. D 49, 3626 (1994); Astropart. Phys. 4, 177 (1995).
- [29] IMB Collaboration, R. Clark et al., The Atmospheric Muon

- Fraction Above 1 GeV, submitted to Phys. Rev. Lett. (Report available at the URL http://beavis.phys.lsu.edu/clark/paper.html .)
- [30] SuperKamiokande Collaboration, K. Young et al., in the Joint APS/AAPT 1997 Meeting, Washington DC, April 1997, to appear in the Proceedings; also available at the URL http://www.phys.washington.edu/~young/superk/drafts/aps97.html .
- [31] LSND Collaboration, W. C. Louis, in *Workshop on Fixed Target Physics at the Main Injector*, Fermi National Accelerator Laboratory, Batavia, Illinois USA, May 1997, to appear in the Proceedings.
- [32] Z. G. Berezhiani and A. Rossi, Phys. Lett. B **367**, 219 (1996).
- [33] K. S. Babu, J. C. Pati, and F. Wilczek, Phys. Lett. B **359**, 351 (1995); **364**, 251(E) (1995).
- [34] S. M. Bilenky, A. Bottino, C. Giunti, and C. W. Kim, Phys. Rev. D 54, 1881 (1996).
- [35] SNO Collaboration, A. Hime et al., in Neutrino Telescopes '96 [2], p. 213.
- [36] KARMEN Collaboration, J. Kleinfeller *et al.*, in *Neutrino '96* [1], to appear in the Proceedings.
- [37] CHORUS Collaboration, D. Saltzberg et al., in Neutrino Telescopes '96 [2] p. 91.
- [38] NOMAD Collaboration, A. Rubbia et al., in Neutrino Telescopes '96 [2] p. 101.
- [39] COSMOS Collaboration, R. A. Sidwell *et al.*, in *Neutrino '96* [1], to appear in the Proceedings.
- [40] A. Ereditato, G. Romano, and P. Strolin, "TENOR: A new experiment for the search of  $\nu_{\mu}$ - $\nu_{\tau}$  oscillations," CHORUS Internal note No. 96-03, 1996 (unpublished); J. J. Gomez-Cadenas and J. A. Hernando, Nucl. Instr. Methods A **381**, 223 (1996).
- [41] CHORUS and NOMAD Collaboration, A. S. Ayan *et al.*, "A high-sensitivity short baseline experiment to search for  $\nu_{\mu} \leftrightarrow \nu_{\tau}$  oscillations, Letter of Intent, CERN Report CERN-SPSC/97-5, 1997 (unpublished).
- [42] Chooz Collaboration Proposal (unpublished); available at the URL h http://duphy4.physics.drexel.edu/chooz.pub/index.htmlx .
- [43] Palo Verde Collaboration Proposal (unpublished); available at the URL http://www.cco.caltech.edu/~songhoon/Palo-Verde/Palo-Verde.html .

## FIGURES

- FIG. 1. Results of the fit to terrestrial neutrino data (90% C.L.) in the scenario 1, for  $m^2=0.45$  eV<sup>2</sup>. Results for  $0.3 \lesssim m^2 \lesssim 0.5$  eV<sup>2</sup> (not shown) are similar.
- FIG. 2. Schematic results of the combined fit to solar and terrestrial neutrino data in the scenario 1.
  - FIG. 3. Implications of the scenario 1 for running and future short-baseline experiments.

------ Accelerator (including LSND) and reactor data
------- Atmospheric sub-GeV and multi-GeV (unbinned) data
------ Combination of all data (90% C.L.)

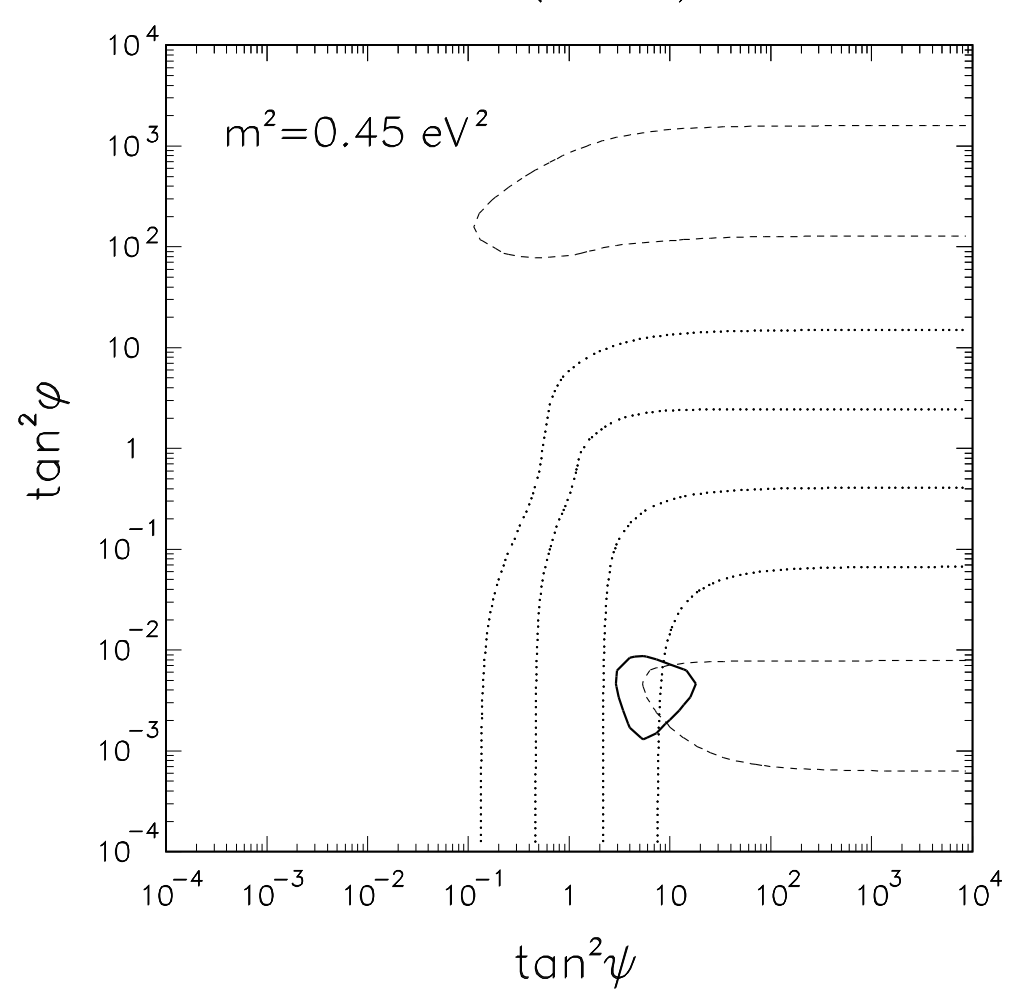


FIG. 1. Results of the fit to terrestrial neutrino data (90% C.L.) in the scenario 1, for  $m^2=0.45$  eV<sup>2</sup>. Results for  $0.3\lesssim m^2\lesssim 0.5$  eV<sup>2</sup> (not shown) are similar.

## Global solution(s) for scenario 1

$$\delta m^{2} = m_{2}^{2} - m_{1}^{2} ; \quad m^{2} = m_{3}^{2} - m_{1,2}^{2}$$

$$\nu_{3} = \sin\varphi \, \nu_{e} + \cos\varphi \left(\sin\psi \, \nu_{\mu} + \cos\psi \, \nu_{\tau}\right)$$

$$\nu_{e} = \cos\varphi \left(\cos\omega \, \nu_{1} + \sin\omega \, \nu_{2}\right) + \sin\varphi \, \nu_{3}$$

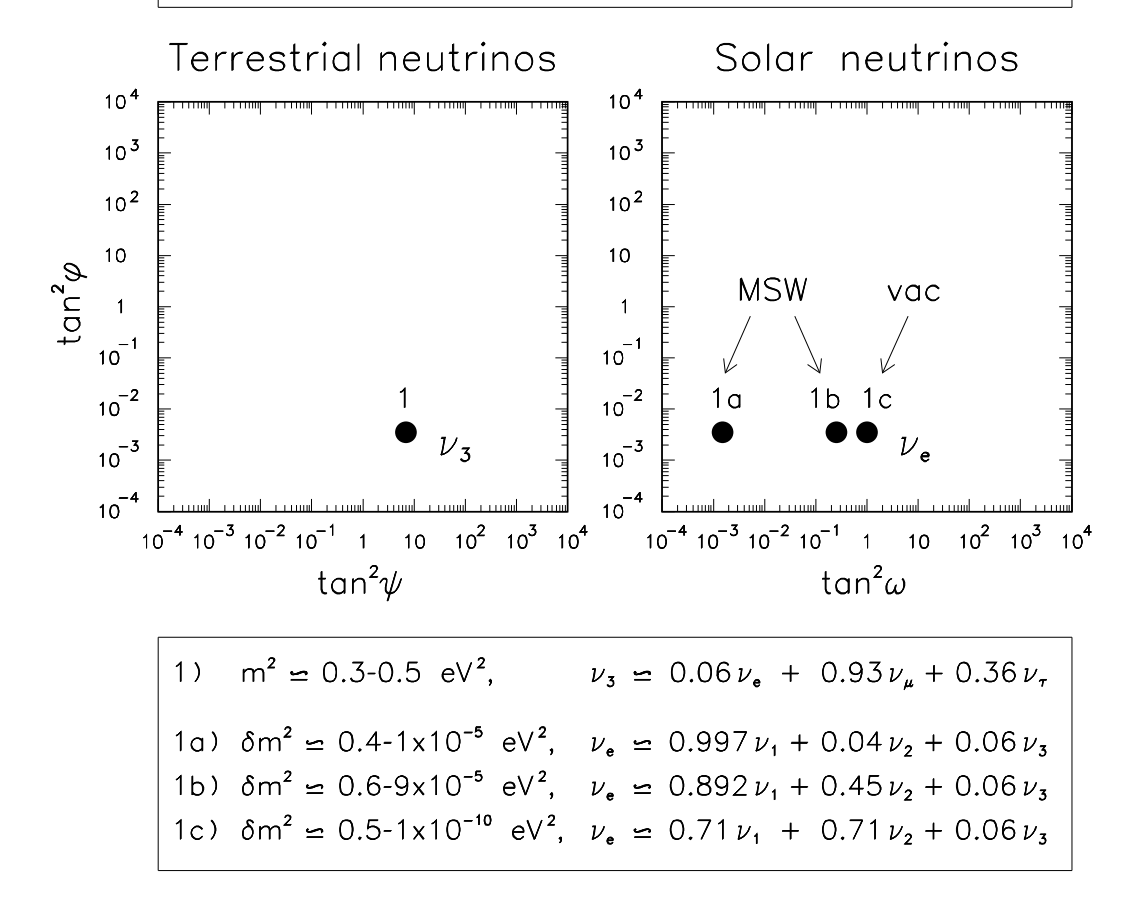


FIG. 2. Schematic results of the combined fit to solar and terrestrial neutrino data in the scenario 1.

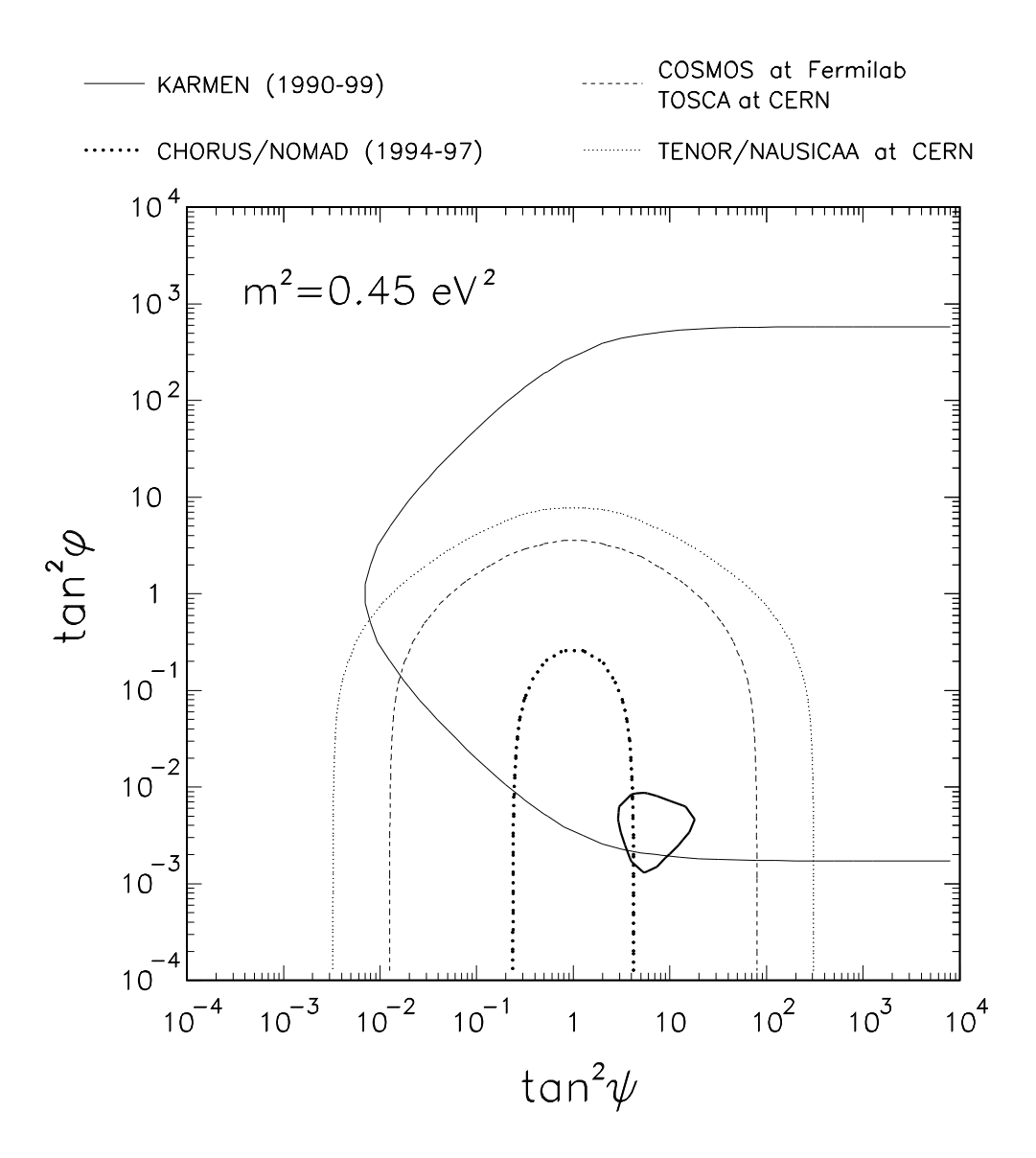


FIG. 3. Implications of the scenario 1 for running and future short-baseline experiments.